

See discussions, stats, and author profiles for this publication at: <https://www.researchgate.net/publication/356884102>

Precipitation temporal repackaging into fewer, larger storms delayed seasonal timing of peak photosynthesis in a semi-arid grassland

Article in *Functional Ecology* · December 2021

DOI: 10.1111/1365-2435.13980

CITATIONS

0

READS

97

7 authors, including:



Joel Aaron Biederman

United States Department of Agriculture

81 PUBLICATIONS 1,837 CITATIONS

[SEE PROFILE](#)



William Kolby Smith

The University of Arizona

79 PUBLICATIONS 3,939 CITATIONS

[SEE PROFILE](#)

Some of the authors of this publication are also working on these related projects:



Ecohydrology [View project](#)



Carbon cycle tracers (COS, 18O-CO₂, SIF) at Biosphere 2 [View project](#)

RESEARCH ARTICLE

Precipitation temporal repackaging into fewer, larger storms delayed seasonal timing of peak photosynthesis in a semi-arid grassland

Fangyue Zhang^{1,2}  | Joel A. Biederman²  | Nathan A. Pierce^{1,2}  | Daniel L. Potts³  | Charles John Devine¹  | Yanbin Hao⁴  | William K. Smith¹ 

¹School of Natural Resources and the Environment, University of Arizona, Tucson, AZ, USA

²USDA Agricultural Research Service Southwest Watershed Research Center, Tucson, AZ, USA

³Biology Department, SUNY Buffalo State, Buffalo, NY, USA

⁴College of Life Sciences, University of Chinese Academy of Sciences, Beijing, China

Correspondence

Fangyue Zhang
Email: fangyuezhong@arizona.edu

Funding information

Strategic Environmental Research and Development Program, Grant/Award Number: RC18-1322; Agricultural Research Service, Grant/Award Number: 58-2022-8-010 and 58-3050-9-013

Handling Editor: Shuli Niu

Abstract

1. Against a backdrop of rising temperature, large portions of the western United States are experiencing fewer, larger and less frequent precipitation events. How such temporal 'repackaging' of precipitation alters the magnitude and timing of seasonal maximum gross primary productivity (GPP_{max}) remains unknown. Addressing this knowledge gap is critical, since changes to GPP_{max} magnitude and timing can impact a range of ecosystem services and management decisions.
2. Here we used a field-based precipitation manipulation experiment in a semi-arid mixed annual/perennial bunchgrass ecosystem with mean annual precipitation ~384 mm to investigate how temporal repackaging of a fixed total seasonal precipitation amount impacts seasonal GPP_{max} and its timing.
3. We found that temporal repackaging of precipitation profoundly influenced the seasonal timing of GPP_{max} . Many/small precipitation events advanced the seasonal timing of GPP_{max} by ~13 days in comparison with climatic normal precipitation. Conversely, few/large events led to deeper soil water infiltration, which delayed the timing of GPP_{max} by up to 16 days in comparison with climatic normal precipitation, and altered end-of-season community composition by increasing the diversity of shallow-rooted annual plants. While GPP_{max} magnitude did not differ across precipitation treatments, it was positively correlated with the abundance and biomass of deeper-rooted perennial bunchgrasses. The sensitivity of plant growth, biomass accumulation and plant life histories to the timing and magnitude of precipitation events and the resulting temporal patterns of soil moisture regulated ecosystem responses to altered precipitation patterns.
4. Our results highlight the sensitivity of semi-arid grassland ecosystem to the temporal repackaging of precipitation. We find that already-observed and model-forecasted shifts toward few/large precipitation events could drive significant delays in the timing of peak productivity for this ecosystem. Adaptive land management frameworks should consider these findings since shifts in peak ecosystem productivity would have major implications for multiple land user communities. Additional research is needed to better understand the role of

climate, community composition and soil properties in mediating variability in the seasonal timing of maximum ecosystem productivity.

KEYWORDS

community composition, maximum photosynthetic production, precipitation repackaging, semi-arid grasslands, vegetation greenness

1 | INTRODUCTION

Climate warming-induced intensification of the hydrologic cycle increases the frequency and intensity of extreme weather events (Dai, 2013; Diffenbaugh et al., 2015). Evidence from across the semi-arid southwestern United States (US) suggests that rainfall regimes are shifting towards larger, less frequent rain events interspersed by longer intervals of days without rainfall (Bradford et al., 2020; Groisman & Knight, 2008; Zhang et al., 2021). However, shifts in the frequency and event size distribution of precipitation have been less well studied than shifts in seasonal or annual totals, and the ecological consequences of such precipitation ‘temporal repackaging’ remain uncertain (Heisler-White et al., 2008; Liu et al., 2017; Potts et al., 2019).

Grassland maximum photosynthetic production (gross primary productivity, GPP_{max}) and its seasonal timing correspond to the magnitude and timing of ecosystem services including carbon sequestration (Xia et al., 2015), plant biomass production for forage and grazing (Hernandez-Ramirez et al., 2011), and erosion control (Zuazo & Pleguezuelo, 2009). Important impacts of GPP_{max} magnitude and timing include management decisions such as animal grazing rotations (Browning et al., 2019; Xu et al., 2016) and possible matches in plant–pollinator biorhythms (Burkle & Alarcón, 2011; Hegland et al., 2009). GPP_{max} is considered as the turning point in vegetation phenophase (i.e. when carbon allocation shifts away from vegetative production and primarily towards structures associated with reproduction), especially for grasslands with clear seasonality. Furthermore, GPP_{max} magnitude and timing are important indicators of seasonal maximum carbon uptake and carbon balance (Niu et al., 2017; Park et al., 2019; Xia et al., 2015). With semi-arid lands playing a dominant role in the trend and variability of the global carbon cycle (Ahlström et al., 2015; Poulter et al., 2014), understanding the mechanisms controlling semi-arid grassland GPP_{max} is not only essential for informed rangeland management, but may also be critical for improving our predictions of grassland carbon cycling in response to global change (Gonsamo et al., 2018).

The precipitation repackaging effect on GPP_{max} magnitude and timing may in large part be determined by the functional traits and the phenology of perennial C4 grasses, the dominant plants in semi-arid rangelands (Bodner & Robles, 2017; Ehleringer et al., 1997). However, changes in water availability due to variations in the amount and timing of rainfall and the resulting depth and magnitude of soil water infiltration can also cause fluctuations in the abundance

of different species within communities (Knapp et al., 2002). Community shifts might be particularly apparent in semi-arid grasslands, which contain mixtures of different plant functional types (e.g. annual, perennial), because the response of grass species to altered precipitation may vary according to their life history (Munson & Long, 2017). Different rooting distributions for different plant functional types in water-limited ecosystems drive the various responses to precipitation repackaging, suggesting a shift in community composition under precipitation repackaging (Liu et al., 2017; Reynolds et al., 2004). These responses may influence seasonal carbon uptake dynamics, since ecosystems harbouring more plant species can achieve higher GPP (Milcu et al., 2014). Few, large rainfall events have relatively deeper infiltration into the soil profile and a lower fraction lost to evaporation compared to smaller rain events, thus proportionally more water is available for plant growth and a higher GPP_{max} (Austin et al., 2004; Guo et al., 2016; Huxman, Snyder, et al., 2004). Additionally, deeper infiltration is expected to favour deeper-rooted perennial plants over shallow-rooted annual grasses and forbs under prolonged dry intervals. Therefore, we expect that temporal repackaging of precipitation will affect seasonal GPP_{max} magnitude and timing. Specifically, in semi-arid grasslands with deep, well-drained soils, few/large events are expected to increase GPP_{max} magnitude and delay GPP_{max} timing.

In the semi-arid rangelands of interior southwestern North America, the majority of ecosystem production occurs between July and September in response to intense, convective rainfall associated with the North American monsoon (Biederman et al., 2017; Hinojo-Hinojo et al., 2019; Scott et al., 2010). Complex interactions between monsoon rainfall variability and the timing of plant growth have limited our ability to predict the magnitude and timing of GPP_{max} in these ecosystems (Briske et al., 2008; Polley et al., 2013). At the regional scale, satellite remote sensing has been used to demonstrate the close relationship between seasonal shifts in vegetation greenness and GPP_{max} magnitude and timing across semi-arid grassland ecosystems (Smith et al., 2019; Yan et al., 2019). Long-term remote sensing observations have further found both the seasonal timing of peak vegetation greenness and peak GPP are largely impacted by seasonal precipitation totals (Yang et al., 2019; Zhou & Jia, 2016), but it remains unclear how the temporal repackaging of precipitation, independent of changes in precipitation totals, may impact vegetation greenness and GPP_{max} magnitude and timing. Identifying patterns and mechanisms of GPP_{max} and its timing in response to precipitation

repackaging have been difficult to discern through long-term observations due to large interannual precipitation variability, legacy and lag effects, and complex impacts of simultaneous variations in natural precipitation amount and temporal packaging (Sala et al., 2012; Wu et al., 2015). However, high degrees of interannual and intra-annual variability in peak vegetation greenness timing suggest that precipitation variability at various time-scales may drive the magnitude and timing of GPP_{max} (Zelikova et al., 2015).

Our objective in this study was to address this knowledge gap by evaluating the impacts of a climatic shift towards fewer and larger precipitation events on the magnitude and seasonal timing of peak photosynthesis. We utilized a new, intensively instrumented field experiment in the semi-arid grassland in Southern Arizona, US, to fully control precipitation over 20 hydrologically isolated plots during the main summer growing season of July–September 2020. We combined measurements of plot-level GPP, vegetation greenness, soil moisture, functional traits, community composition to address the following questions: (a) What is the impact of precipitation repackaging on seasonal GPP_{max} magnitude and timing? and (b) How is the relationship between precipitation repackaging and GPP_{max} mediated by plant functional traits and community composition?

2 | MATERIALS AND METHODS

2.1 | Site description

This experiment was conducted at the experimental facility named Rainfall Manipulation in the Santa Rita Experimental Range (RainManSR; 31.79°N, 110.90°W, 1,075 m a.s.l.). The mean annual temperature (2004–2018) is approximately 19.0°C, with daytime maximum temperature often exceeding 35°C in June (Scott et al., 2009). The mean annual precipitation (2004–2018) is 384 mm, about 50%–60% of which arrives during the summer growing season associated with the North American Monsoon (July–September) (Roby et al., 2020; Scott et al., 2008). Soils at the site are deep, well-drained sandy loams (72% sand, 13% clay, and 15% silt) and do not vary considerably across the site, where all experimental plots were within 140 m of one another. The extant ecosystem is savanna, with widely spaced *Prosopis velutina*, *Senegalia greggii* and *Celtis pallida* the most common woody species and a sparse understory of C4 perennial bunchgrasses (*Eragrostis lehmanniana*, *Digitaria californica*, *Heteropogon contortus*) interspersed with a seasonally dynamic community of C4 annual grasses (*Bouteloua barbata*, *B. aristoides*, *Aristida adscensionis*) and C3 forbs (*Evolvulus arizonicus*, *Solanum elaeagnifolium*, *Eriogononum abertianum*, *Machaeranthera tanacetifolia*). The field research was conducted with permission from the University of Arizona Agricultural Experiment Station, Accession No. 19-66, granted 8 May 2019 under a cooperative agreement between the University of Arizona and the USDA-Agricultural Research Service (agreement no. UA-3030310).

2.2 | Rain-exclusion shelter design

The experiment used a randomized block design, with each of five rainout shelters considered a block, and four plots, measuring 1.2 m × 1.5 m, spatially randomized under each shelter. Shelters are of a semi-circular 'hoop house' design with dimensions of 4.3 m width, 22 m length and 2.5 m maximum height (GrowSpan Greenhouse Structures), and were covered with transparent, 6-mil polyethylene greenhouse film that transmits 92% of photosynthetically active radiation (Lumite, Inc.). Hardware fabric (1.2 cm mesh) was installed around each shelter to a height of 1 m and a sub-surface depth of 0.3 m to deter rodent and lagomorph disturbance within the shelters yet allow access for small reptiles, arthropods and soil macroinvertebrates. There were negligible environmental impacts from the rainout shelters, which caused minimal change in relative humidity and air temperature (Figure A1). Each shelter was fashioned with gutters to divert precipitation to a storage tank; this harvested rainwater was used for all irrigation treatments.

To hydraulically isolate plots above-ground and below-ground, plots were trenched on all sides to a depth of 80 cm, and soil columns were lined with black, 6-mil polyethylene film that extended to the trench bottoms before backfilling. Plots were also lined with 0.25 mm galvanized steel flashing that extended 50 cm down the soil column and 10 cm above the soil surface.

To provide a relatively consistent initial plant community among plots in this typically patchy, heterogeneous desert grassland, we transplanted seedlings of a native perennial bunchgrass (*Digitaria californica* (Benth.) Henrard) at a density of approximately 20 plants per m² in November 2019. From transplant through 1 May 2020, each plot received supplementary irrigation to promote establishment approximately biweekly. No irrigation was applied during May and June 2020, in accord with the normal local climatic rainfall pattern. Establishment of *Digitaria californica* transplant seedlings varied, providing a range of abundance and biomass, which proved useful in testing their importance as predictors of GPP.

2.3 | Experimental setup

The precipitation treatments were carried out during July–September 2020 (Figure 1). This experiment only altered the dry interval duration and frequency of precipitation events, while maintaining constant monsoon season precipitation of 205 mm, equivalent to the ~45-year mean (1975–2019). Within the context of a 45-year climate record for this location (Figure A2), the durations of dry intervals were fixed for each precipitation treatment as follows: 3.5 days (S1), 7 days (S2, climatic normal average dry interval between events), 14 days (S3) and 21 days (S4). Precipitation events were simulated by a digital flow meter (A109GMN025NA1; Assured Automation) using collected rainwater. Events larger than 7 mm were applied in multiple small doses over 30–60 min to prevent ponding. All plots received 38 mm on 14 July 2020, providing all treatments with sufficient moisture to initiate the summer monsoon growing

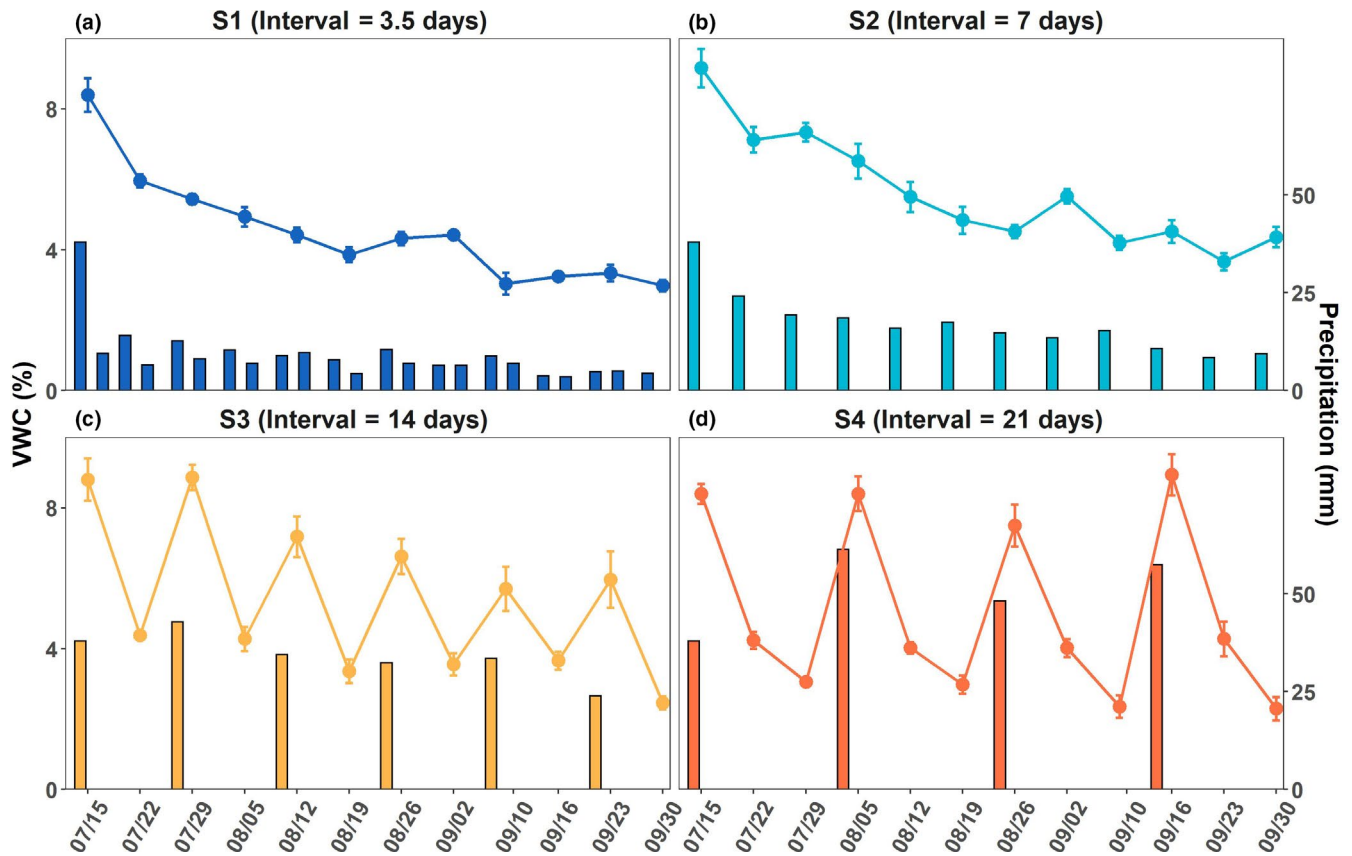


FIGURE 1 Experimental precipitation applications (mm, bars) and weekly soil volumetric water content (VWC, %, lines) at 10 cm depth during experiment

season. Thereafter, the mean (range) precipitation event sizes during the experimental period were 9 (4–14) mm for S1, 17 (8–24) mm for S2, 34 (24–43) mm for S3 and 51 (48–61) mm for S4.

2.4 | Data collection

2.4.1 | Soil moisture and temperature

Soil moisture in the top 10 cm was measured weekly in each plot using a HydroSense II soil water content sensor (12 cm tines, CS659; Campbell Scientific). In nine selected plots, half-hourly soil moisture and temperature at three depths were measured by sensors (12 cm tines, CS655; Campbell Scientific) inserted from the soil surface at a 30° from nadir, providing an integrated measurement over the top 10 cm of soil, and horizontally into the soil column at 25 and 75 cm depths. Due to cost constraints for the sensors, we prioritized the extreme treatments (S1 and S4) and the intermediate treatment S2. Given the highly dynamic nature of soil moisture in pulse-driven desert ecosystems, seasonal mean soil moisture is often not representative of plant stress. Therefore, we quantify the persistence of ‘wet soil’ (defined here as soil moisture $>0.05 \text{ m}^3/\text{m}^3$, determined by in situ measurements to correspond to soil water potential $>-1 \text{ MPa}$ at this site) at three depths in the soil using cumulative distribution curves at daily scale (average of half-hourly soil moisture).

2.4.2 | Ecosystem CO_2 fluxes

We measured whole-plot CO_2 fluxes with a closed static chamber (1.3 m wide, 1.0 m tall, 1.6 m long), using an infrared gas exchange analyser configured for closed-loop measurements (IRGA; LI-6400; Li-Cor Inc.) fitted inside (Huxman, Cable, et al., 2004; Potts et al., 2006). During the measurement, the analyser was mounted on a tripod, and two 15 cm diameter fans ran continuously to mix the air inside the chamber. The chamber was constructed of a PVC pipe frame and a tightly sewn polyethylene sheet which was sealed around the plot base by a heavy steel chain. After the chamber atmosphere was thoroughly mixed by the fans for 30 s after the chamber was sealed, CO_2 concentration measurements were taken at 2-s intervals during a 90-s period. Linear fits of CO_2 concentration were used to calculate net ecosystem exchange (NEE). Following NEE measurement, the chamber was vented, then reset and covered with an opaque cloth, and the CO_2 exchange measurements were repeated. Because the second set of measurements eliminated light (and hence photosynthesis), the values obtained represent ecosystem respiration (ER). GPP was calculated by the difference between ER and NEE.

We calculated CO_2 fluxes (F_c , $\mu\text{mol m}^{-2} \text{ s}^{-1}$) for each individual plot measurement with the method reported by Jasoni et al. (2005) and Steduto et al. (2002) using Equation (1):

$$F_c = \frac{VP_{av} (1,000 - W_{av})}{RS (T_{av} + 273)} \times \frac{dC}{dt}, \quad (1)$$

where V is the volume of chamber (m^3); P_{av} the average pressure (KPa) during measurement period; W_{av} the average water mole fraction (mmol/mol) during measurement period; R the ideal gas constant ($8,314 \text{ J mol}^{-1} \text{ K}^{-1}$); S the surface area covered by chamber (m^2); T_{av} the average temperature ($^{\circ}\text{C}$); C is the mole fraction of CO_2 ($\mu\text{mol/mol}$); and $\frac{dC}{dt}$ is the slope of linear regression of C on time. The flux measurements were made weekly during the morning (9:00–12:30) on sunny days.

2.4.3 | Plot-level phenology observations

In each plot, plant phenology and whole-plot greenness were tracked using half-hourly photographs taken during the daylight hours between 9:00 a.m. and 4:00 p.m. using Raspberry Pi Camera Module V2 (Raspberry Pi Foundation). These cameras were configured to maintain a fixed white balance and were mounted above each plot under a steel weather shield to prevent them from overheating in direct sunlight. Each camera captured the full area of two adjacent plots and maintained a static, nadir-oriented field of view. Using the PHENOPIX package (Filippa et al., 2016), we defined a region of interest (ROI) for each plot that included only the vegetated area inside the aluminium flashing. We then calculated green chromatic coordinate (GCC) for all pixels within the ROI and averaged all pixel GCC values to obtain plot-scale GCC value for each half-hourly image (Filippa et al., 2016). Finally, daily GCC estimates were extracted as the 90th percentile of all half-hourly GCC values for a given day following a standard method for minimizing changes in hourly illumination condition (Yan et al., 2019). GCC was calculated as follows:

$$\text{GCC} = \frac{G}{(R + G + B)}, \quad (2)$$

where R , G and B are the red, green and blue layers of the image, respectively.

2.4.4 | Community structure and plant functional traits

We measured plant species richness (total number of species) and Shannon diversity (number of individuals of each species) on 1 August and 3 October 2020, using a $1 \text{ m} \times 1 \text{ m}$ quadrat centred inside each plot. In October 2020, for each living *Digitaria californica* plant in each plot, plant height was defined by the highest leaf collar when its culm was shifted perpendicular to the soil surface. The number of vegetative culms and reproductive culms were also counted for each live plant. Basal diameter was determined by measuring the widest diameter and its perpendicular diameter with calipers. The biomass of each *Digitaria californica* individual was estimated by allometry (3) (Nafus et al., 2009):

$$b = \frac{1}{e^{3.51}} d^{0.963} h^{1.353}, \quad (3)$$

where b is the plant biomass, d is the diameter and h is the height.

2.5 | Data analysis

We used a cubic smoothing spline to interpolate the GPP time series to a 1-day resolution (Chen et al., 2006; Cong et al., 2012). Then we calculated the GPP_{max} magnitude and timing. The effects of precipitation repackaging on GPP_{max} were assessed using mixed-effects models by the 'lme' function in the NLME package (Pinheiro et al., 2021), where precipitation treatment was fixed effect and block was random. Significant differences were identified using analysis of variance and p values, followed by a Duncan's test to compare the effects for each treatment. Species richness and Shannon diversity index (H) in August and October were compared with a paired t test. Regression analysis was used to explore relationships between GPP_{max} , GPP_{max} timing, plant functional traits, community composition changes, and GCC_{max} and GCC_{max} timing. All analyses were conducted in R version 4.0.2 (R Core Team, 2013).

3 | RESULTS

3.1 | Gross primary productivity dynamics

Across the rainfall treatments, the seasonal dynamics of GPP followed a single-peak pattern during the summer monsoon growing season (Figure 2a). Rainfall treatment did not significantly influence GPP_{max} magnitude ($p = 0.40$, Figure 2b), while the timing of GPP_{max} varied significantly with rainfall treatment ($p < 0.01$, Figure 2c). The earliest peak in seasonal GPP occurred in the S1 treatment (many/small events) while the latest seasonal peak in GPP occurred in the S4 treatment (few/large events; Figure 2c, 27.0 ± 2.9 and 56.4 ± 1.1 days after first irrigation, respectively). As compared to normal conditions (S2, 40.4 ± 5.3 days), many/small events (S1) brought GPP_{max} timing forward by 13 days, while few/large events (S4) shifted GPP_{max} later by 16 days (Figure 2c).

3.2 | Green chromatic coordinate dynamics

We observed no significant effects of precipitation repackaging on the magnitude of maximum GCC (GCC_{max} , $p = 0.77$, Figure 3a). However, in comparison with the climatic normal precipitation pattern of the S2 treatment, the seasonal timing of GCC_{max} was significantly delayed with few/large events in the S4 treatment ($p < 0.05$, Figure 3b). The GCC_{max} magnitude showed marginally positive relationships with GPP_{max} ($p = 0.07$, Figure 3c), and GCC_{max} timing showed a significant positive relationship with GPP_{max} timing ($p < 0.01$, Figure 3d).

3.3 | Soil moisture dynamics

Compared to the climatic normal precipitation pattern (S2, $5.6 \pm 0.6\%$), time-averaged weekly soil moisture at 10 cm depth

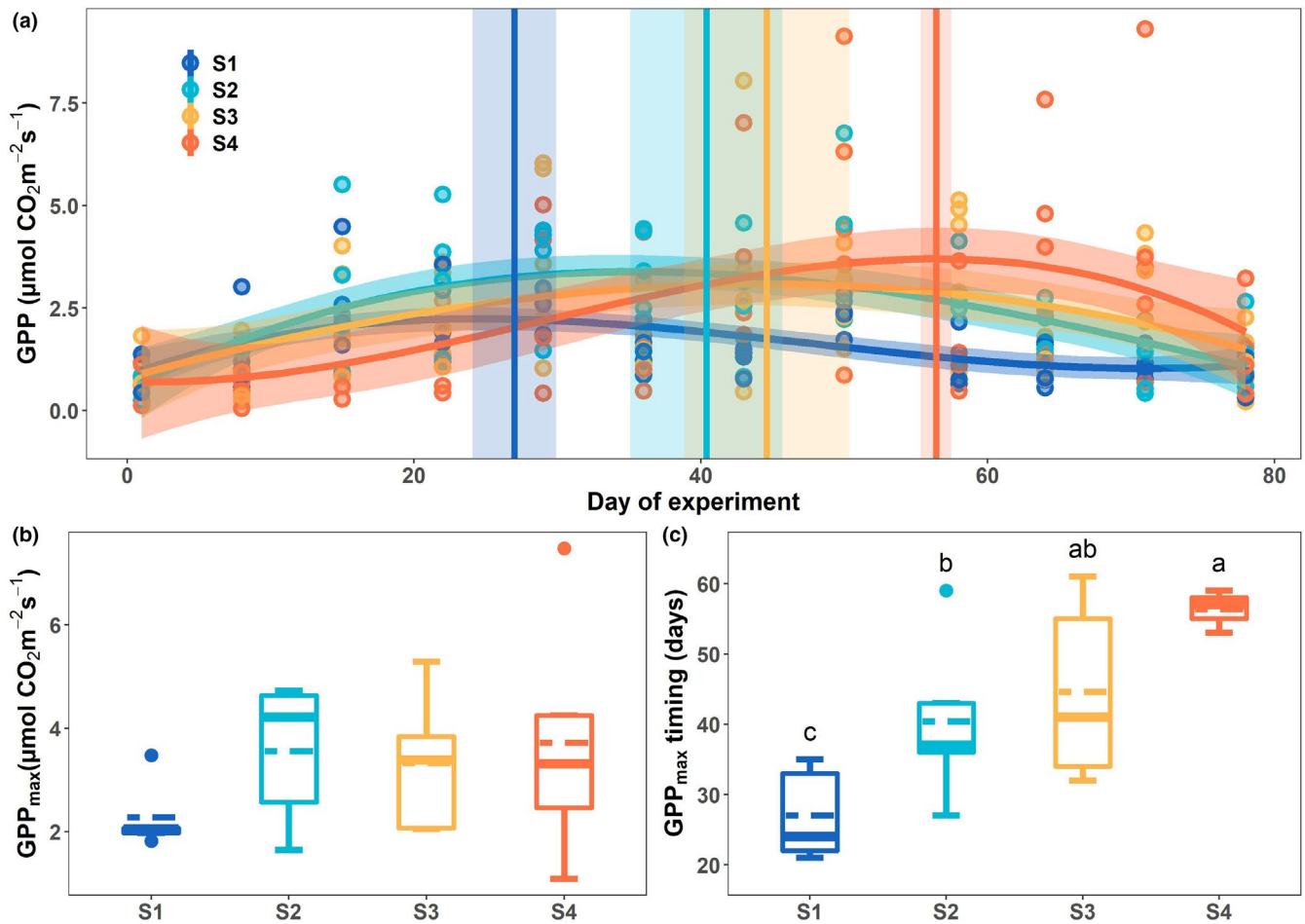


FIGURE 2 Weekly measurements of gross primary production (GPP) for four treatments during the summer monsoon growing season (a). Vertical lines indicate the timing of peak GPP (GPP_{max}). GPP_{max} magnitude (b) and GPP_{max} timing (days since beginning of irrigation treatments, (c) under each temporal packaging treatment. Dashed lines indicate the average of each treatment. Significant treatment differences are indicated by different letters ($p < 0.05$) among treatments

was significantly lower ($p < 0.01$) under many/small events (S1, $4.5 \pm 0.1\%$) and few/large events (S4, $5.0 \pm 0.2\%$) (Figure 1).

The cumulative days of surface (0–10 cm) wet soil were 23 in S1 and 29 in S4, which are both much lower than the cumulative days with wet soil under the intermediate climatic normal precipitation pattern (S2, 47 days) (Figure 4a), although treatment differences were only marginally significant ($p = 0.06$). The many/small events in S1 treatment accumulated only 3 days with wet soil at the 25 cm depth and none at the 75 cm depth (Figure 4b,c). In contrast, few/large events in the S4 treatment resulted in 27 days of wet soil at 25 cm depth and 38 days at 75 cm depth (Figure 4c).

3.4 | Plant functional traits

Digitaria californica abundance, its biomass and height per plant in the plot explained significant variability ($p < 0.05$) in GPP_{max} magnitude across all treatments (Figure A3). At the end of growing season, the few/large events in the S4 treatment increased reproductive culms of each plant significantly ($p < 0.05$), with 4.0 ± 1.1 culms

per plant, compared to the climatic normal precipitation pattern (S2, 1.7 ± 0.3 culms per plant, Figure 5a). Although GPP_{max} timing of the different treatments was not related to *Digitaria californica* abundance, biomass or height (Figure A4), the average number of *Digitaria californica* reproductive culms per plant was positively correlated with GPP_{max} timing ($p < 0.05$, Figure 5b).

3.5 | Community structure dynamics

Few/large events every 2 or 3 weeks in the S3 and S4 treatments caused increases in annual grass species richness between August and October ($p < 0.01$ and $p < 0.05$, respectively, Figure 6a). Except for S1 (many/small events), plots in the other three treatments showed increased annual grass community Shannon diversity between August and October ($p < 0.05$, Figure 6b). In addition, many/small events in the S1 treatment were associated with a statistically marginal decline in perennial forb richness between August and October ($p < 0.1$, Figure 6c). Few/large events in S4 treatments also increased community species richness and

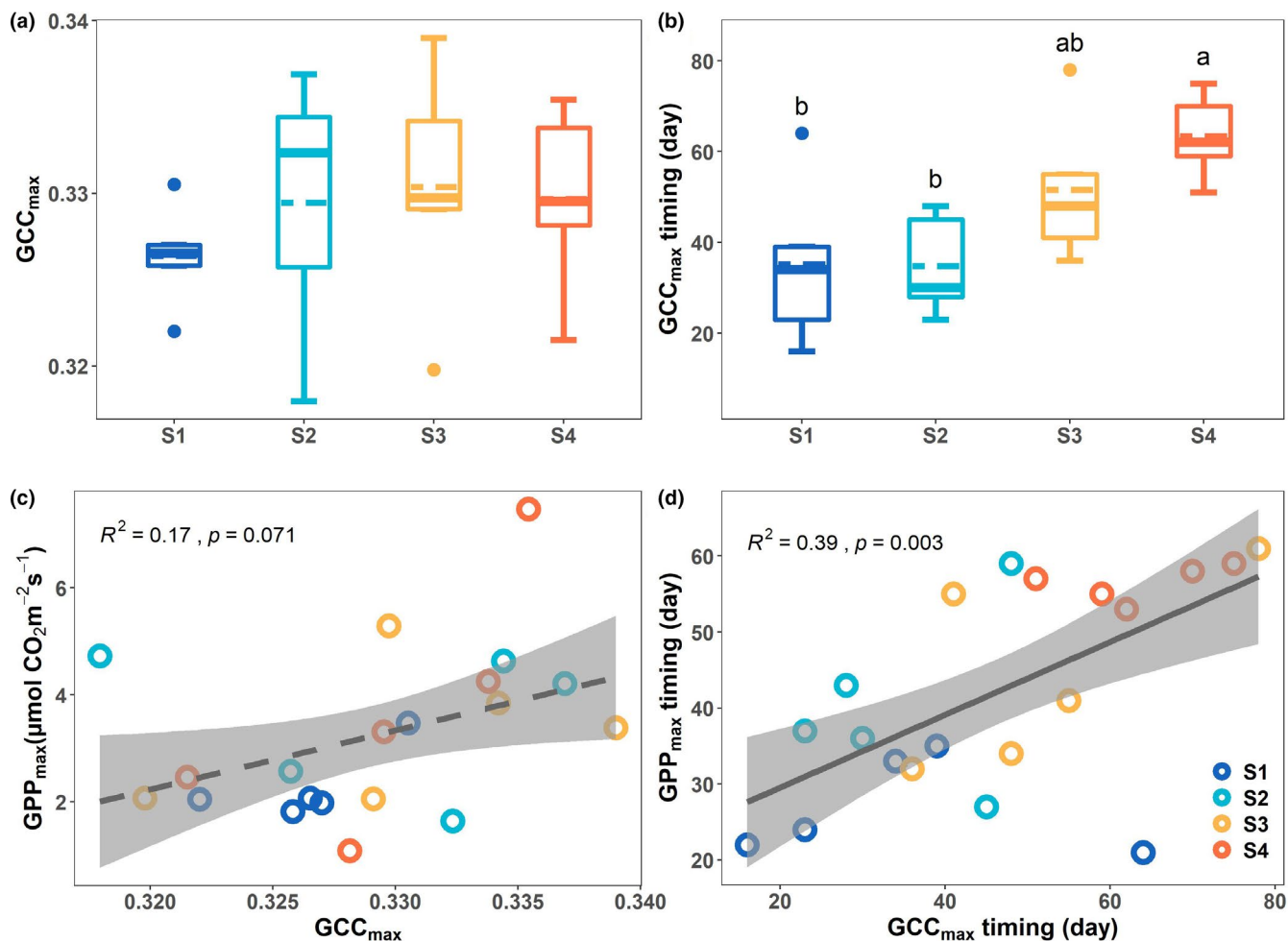


FIGURE 3 Seasonal maximum green chromatic coordinates (GCC_{max} , a) and GCC_{max} timing (days since beginning of irrigation treatments, b) under each temporal packaging treatment. Significant treatment differences are indicated by letters ($p < 0.05$). Relationships between magnitudes of maximum gross primary productivity (GPP_{max}) and GCC_{max} (c) and between timing of each maximum (d)

Shannon diversity in October than the diversity in August (Figure A5a,b). Across precipitation repackaging treatments, seasonal differences (October minus August) in annual grass species richness and Shannon diversity, community species richness and Shannon diversity were positively correlated with GPP_{max} timing ($p < 0.01$, Figure 6d,e, Figure A5c,d).

4 | DISCUSSION

Precipitation variability and the frequency of extreme-duration drought events are increasing and are forecasted to continue to increase with climate warming (Bradford et al., 2020; Zhang et al., 2021). Understanding the impacts these hydroclimate changes will have on semi-arid ecosystems is critical given the significant role that water-limited systems have in the global carbon cycle and global resource availability (Ahlström et al., 2015). Our study showed that temporal repackaging of a fixed seasonal precipitation total had significant impacts on semi-arid grassland seasonal GPP_{max} timing. Specifically, fewer and larger precipitation events delayed the

GPP_{max} timing in comparison to the climatic normal precipitation pattern (Figure 2). The seasonal peak of plot-level canopy greenness (i.e. GCC_{max}) was also delayed by a shift towards fewer and larger precipitation events (Figure 3). These shifts in GPP_{max} and GCC_{max} timing were associated with temporal variability in accumulated soil moisture at various rooting depths (Figure 4), the production of reproductive tillers of perennial grasses (Figure 5) and intra-seasonal shifts in plant community richness and Shannon diversity (Figure 6). Taken together, these results describe the sensitivity of the timing of both maximum photosynthetic production and peak vegetation greenness in semi-arid grasslands to already-observed and model-forecasted shifts in intra-annual rainfall variability leading to less frequent and larger precipitation events.

In semi-arid ecosystems, larger storms tend to wet the entire root zone, and these soil moisture pulses are main drivers of plant growth and ecosystem function (Huxman, Cable, et al., 2004; Noy-Meir, 1973). Likewise, we observed more abundant moisture at 75 cm soil depth in the S4 rainfall treatment, which was characterized by few/large rainfall events (Figure 4). Coincident with a greater soil moisture availability in deeper soil layers, the

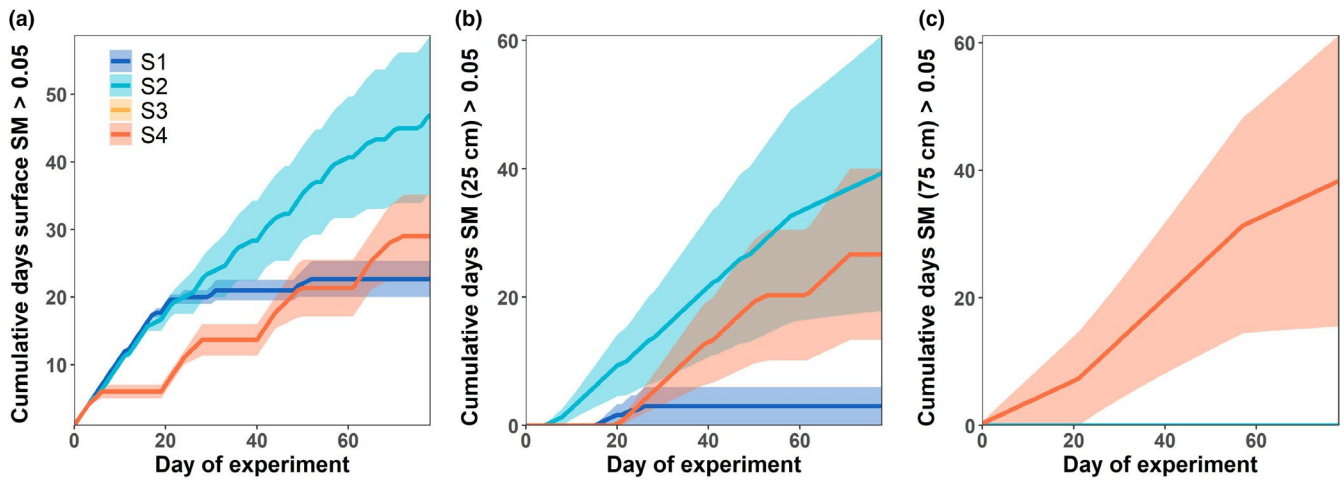


FIGURE 4 Cumulative days of 'wet soil' defined as soil moisture (SM) > 0.05 m³/m³ in the 0–10 cm surface soil (a), at depth 25 cm (b) and 75 cm (c). Shadows represent the standard error of the mean ($n = 3$)

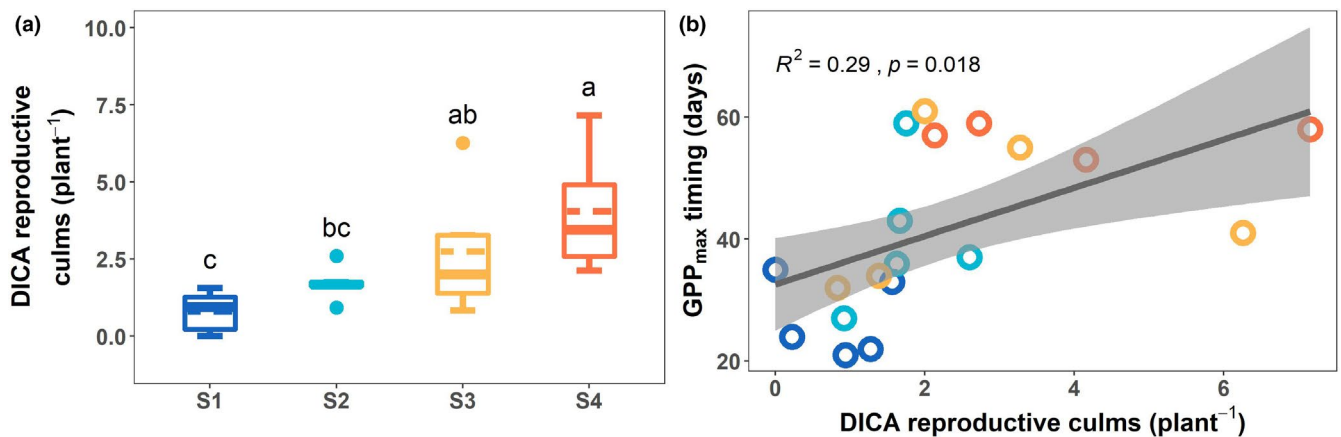


FIGURE 5 *Digitaria californica* (DICA) reproductive culms of each plant under each treatment (a). Dashed lines indicate the average of each treatment. Significant treatment differences are indicated by different letters ($p < 0.05$) among treatments. Correlations of seasonal maximum gross primary production (GPP_{max}) timing with *Digitaria californica* reproductive culms of each plant (b). Each point represents a plot, rainfall treatments are indicated by colour following the notation presented in Figure 3d

production of reproductive culms by *Digitaria californica* increased as precipitation events became less frequent and larger, which supports the link between rainfall variability and sexual reproduction in perennial grasses (Figure 5a; Munson & Long, 2017). Moreover, high photosynthetic capacity of successive leaves during reproductive growth may lead to increased total plant productivity (Woledge, 1978) which may contribute to the observed correlation between *Digitaria californica*'s reproductive culm production and the GPP_{max} timing (Figure 5b). In our study, longer intervals between precipitation events increased soil surface temperatures (Figure A6) and exacerbated plant water stress, with negative consequences for plant growth, especially annual grasses, at the beginning of monsoon (Figure 6). Annual plants in arid environments are often able to resume rapid growth following large storms, a behaviour that could provide competitive advantage under unpredictable rainfall patterns, tending to stabilize biomass in highly variable climates (Gutierrez et al., 1988; Miranda et al., 2009).

The nearly 2 weeks advance of GPP_{max} timing with more-frequent/smaller events might be a consequence of the decreasing perennial forbs diversity during the late growing season. Perennial forbs often have taproot systems that are generally in deeper portions of the soil profile, whereas the annual grasses are shallow-rooted (Gibbens & Lenz, 2001; Kurc & Small, 2007). Frequent, small precipitation events that wet the soil surface without infiltrating the deeper rooting zone of perennials (Fay et al., 2008; Liu et al., 2017) may mainly stimulate physiological activity of the most shallowly rooted annuals. Given the limited storage capacity of the shallowest soil layers as well as their rapid depletion by evaporation, we suggest the many/small events in S1 treatment constrained moisture availability for more deeply rooted perennials, thereby contributing to an advancement in the seasonal timing of GPP_{max}.

Our findings were robust across both plot-level GPP and GCC estimates, which together provide convincing support for the idea

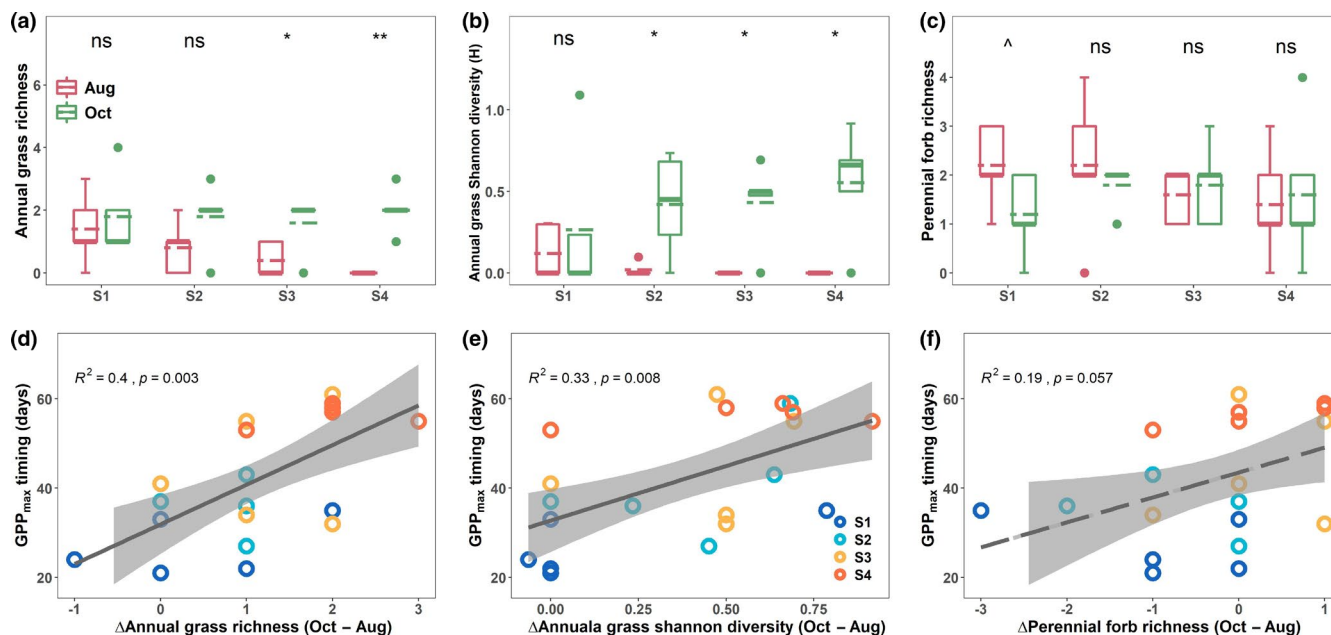


FIGURE 6 Annual grass species richness (a), Shannon diversity index (b) and perennial forb species richness (c) in August (red) and October (green) under different treatments. The significance of the differences between August and October is indicated as ** $p < 0.01$, * $p < 0.05$, $\wedge p < 0.1$. The relationships of monsoon maximum gross primary production (GPP_{max}) timing with differences between October and August values of annual grass richness (d), Shannon diversity (e) and perennial forb richness (f)

that precipitation repackaging will drive significant shifts in the seasonal trajectory of vegetation productivity. Changes in GCC closely followed GPP dynamics across treatments (Figure 3), suggesting that ecosystem greenness state is a key determinant of vegetation carbon uptake in semi-arid grasslands. This finding is consistent with a previous study that found tower-based measurements of ecosystem GCC were closely correlated with ecosystem-scale GPP for a semi-arid grassland site also located in the Santa Rita Experimental range (Yan et al., 2019). Our results demonstrate the value of coupled plot-level imaging and gas exchange measurements at high temporal frequency for monitoring the seasonal productivity dynamics of semi-arid grasslands (Shiklomanov et al., 2019).

Although there were no statistically significant differences in GPP_{max} magnitude under temporal repackaging of precipitation, the positive relationships between GPP_{max} and several measures of *Digitaria californica* structural traits demonstrate the contribution of perennial bunchgrasses to overall productivity in this ecosystem (Figure A3). These results are consistent with observations from East Asian grasslands which indicated that the vegetation biomass is the controlling factor on ecosystem productivity (Fang et al., 2018; Nakano et al., 2008). Vegetation height was related to the curvature of the light response curve and identified as a significant predictor of canopy net ecosystem CO₂ exchange (Milcu et al., 2014). Additionally, the dominant plant abundance was also related to GPP_{max} (Figure A3), possibly because *Digitaria californica* has relatively high photosynthetic capacity and productivity due to its large size, high leaf area and deep roots, which provide advantage in competition for limited water and nutrients (Grime, 2006). Seasonal soil temperatures at both 10 and 25 cm depths were also

positively correlated with GPP_{max} magnitude in our study (Figure A7), consistent with the idea that soil temperature potentially regulates CO₂ flux in semi-arid grasslands (Wang et al., 2011). Our finding that relatively frequent, smaller events had lower GPP_{max} and GCC_{max} than the climatic normal precipitation patterns (although no significant effects were identified, Figures 2b and 3a) partly supports a previous finding that CO₂ fluxes declined under relatively high-frequency precipitation events over a 4-year experiment in a temperate grassland (Liu et al., 2017). Future work is required to explore how GPP_{max} magnitude may respond to precipitation temporal repackaging in arid and semi-arid ecosystems spanning a range of mean annual temperature and precipitation, which has been shown to further mediate ecosystem responses to increasing interannual variability of precipitation (Hou et al., 2021).

The many/large events treatment (S3) did not produce measurable effects on either GPP_{max} or GPP_{max} timing relative to the climatological mean rainfall treatment (S2), which implies that the plant community is adapted to a range of short-term precipitation variability. The rainfall events in S3 treatment, while larger than the climatic normal S2, might not have been large enough to elicit impactful changes in deeper-root plant activity or to substantially change the fraction of precipitation lost to evaporation (Schwinning et al., 2003).

Here we not only reveal how seasonal GPP_{max} and its timing are responding to precipitation repackaging, important for grassland carbon cycling, but also how community structure is expected to respond to the growing duration of drought intervals expected between rainfall events (Zhang et al., 2021). Although our study shines a light on how GPP_{max} timing is delayed under

more extreme-duration drought, more monitoring is needed to fully capture seasonal GPP changes that result from precipitation repackaging (e.g. the start of the green-up or dry-down of canopy, seasonal GPP length). To accomplish these goals, the combining of high-frequency plot imaging and plot-level gas exchange are needed to track pulse dynamics which are important in controlling semi-arid vegetation dynamics (Huxman, Snyder, et al., 2004). As soil nutrient requirements and wetting/drying cycles may constrain the responses of plant activity and soil microbes to precipitation pulses (Potts et al., 2006), our future work will also focus on daily dynamics following pulses to better understand the factors driving differences across treatments.

5 | CONCLUSIONS

Our results indicate that the seasonal GPP_{max} timing in a semi-arid grassland can be quite responsive to precipitation temporal repackaging. Temporal repackaging of rainfall into few events with correspondingly long dry intervals postpones peak photosynthesis, while maintaining the magnitude of GPP_{max} , compared with historically normal precipitation patterns. Moreover, few/large precipitation events may influence the timing of maximum canopy greenness and the seasonal dynamics of community composition. While GPP_{max} magnitude was not sensitive to precipitation repackaging, few/large precipitation patterns may promote deeper-rooted perennial plants which are resilient to future extreme-duration drought. Accurately forecasting how semi-arid ecosystem GPP_{max} magnitude and timing respond to climate change, and consequently their impact on the global carbon budget or optimizing resources availability, will require knowledge of how the magnitude, frequency and timing of precipitation might be altered in the future.

ACKNOWLEDGEMENTS

We acknowledge the support for this work provided by the Strategic Environmental Research and Development Program (SERDP; project number RC18-1322), the United States Department of Agriculture (USDA; cooperative agreement numbers 58-3050-9-013 and 58-2022-8-010) and the University of Arizona Earth Dynamics Observatory, funded by the office of Research, Innovation & Impact. Any use of firm, product or trade names is for descriptive purposes only and does not imply endorsement by the U.S. Government. USDA is an equal opportunity employer.

CONFLICT OF INTEREST

The authors declare no conflicts of interest or competing interests.

AUTHORS' CONTRIBUTIONS

J.A.B. and W.K.S. conceived and designed the study; F.Z., N.A.P. and C.J.D. collected the data for manipulative experiment; F.Z. carried out statistical analyses and wrote the first version of the manuscript; J.A.B., N.A.P., D.L.P., C.J.D., Y.H. and W.K.S. edited the manuscript

and all authors contributed critically to the drafts and gave final approval for publication.

DATA AVAILABILITY STATEMENT

Data available from the University of Arizona Research Data Repository <https://doi.org/10.25422/azu.data.16823602> (Zhang et al., 2021).

ORCID

Fangyue Zhang  <https://orcid.org/0000-0002-5479-6214>

Joel A. Biederman  <https://orcid.org/0000-0002-1831-461X>

Nathan A. Pierce  <https://orcid.org/0000-0003-2798-5455>

Daniel L. Potts  <https://orcid.org/0000-0002-1757-3484>

Charles John Devine  <https://orcid.org/0000-0003-1651-7613>

Yanbin Hao  <https://orcid.org/0000-0001-6821-0395>

William K. Smith  <https://orcid.org/0000-0002-5785-6489>

REFERENCES

- Ahlström, A., Raupach, M. R., Schurgers, G., Smith, B., Arneth, A., Jung, M., Reichstein, M., Canadell, J. G., Friedlingstein, P., Jain, A. K., Kato, E., Poulter, B., Sitch, S., Stocker, B. D., Viovy, N., Wang, Y. P., Wiltshire, A., Zaehle, S., & Zeng, N. (2015). The dominant role of semi-arid ecosystems in the trend and variability of the land CO₂ sink. *Science*, 348(6237), 895. <https://doi.org/10.1126/science.aaa1668>
- Austin, A. T., Yahdjian, L., Stark, J. M., Belnap, J., Porporato, A., Norton, U., Ravetta, D. A., & Schaeffer, S. M. (2004). Water pulses and biogeochemical cycles in arid and semiarid ecosystems. *Oecologia*, 141(2), 221–235. <https://doi.org/10.1007/s00442-004-1519-1>
- Biederman, J. A., Scott, R. L., Bell, T. W., Bowling, D. R., Dore, S., Garatuzo-Payan, J., Kolb, T. E., Krishnan, P., Krofcheck, D. J., Litvak, M. E., Maurer, G. E., Meyers, T. P., Oechel, W. C., Papuga, S. A., Ponce-Campos, G. E., Rodriguez, J. C., Smith, W. K., Vargas, R., Watts, C. J., ... Goulden, M. L. (2017). CO₂ exchange and evapotranspiration across dryland ecosystems of southwestern North America. *Global Change Biology*, 23(10), 4204–4221. <https://doi.org/10.1111/gcb.13686>
- Bodner, G. S., & Robles, M. D. (2017). Enduring a decade of drought: Patterns and drivers of vegetation change in a semi-arid grassland. *Journal of Arid Environments*, 136, 1–14. <https://doi.org/10.1016/j.jaridenv.2016.09.002>
- Bradford, J. B., Schlaepfer, D. R., Lauenroth, W. K., & Palmquist, K. A. (2020). Robust ecological drought projections for drylands in the 21st century. *Global Change Biology*, 26(7), 3906–3919. <https://doi.org/10.1111/gcb.15075>
- Briske, D. D., Derner, J. D., Brown, J. R., Fuhlendorf, S. D., Teague, W. R., Havstad, K. M., Gillen, R. L., Ash, A. J., & Willms, W. D. (2008). Rotational grazing on rangelands: Reconciliation of perception and experimental evidence. *Rangeland Ecology & Management*, 61(1), 3–17. <https://doi.org/10.2111/06-159R.1>
- Browning, D. M., Snyder, K. A., & Herrick, J. E. (2019). Plant phenology: Taking the pulse of rangelands. *Rangelands*, 41(3), 129–134. <https://doi.org/10.1016/j.rala.2019.02.001>
- Burke, L. A., & Alarcón, R. (2011). The future of plant-pollinator diversity: Understanding interaction networks across time, space, and global change. *American Journal of Botany*, 98(3), 528–538. <https://doi.org/10.3732/ajb.1000391>
- Chen, J. M., Deng, F., & Chen, M. (2006). Locally adjusted cubic-spline capping for reconstructing seasonal trajectories of a satellite-derived surface parameter. *IEEE Transactions on Geoscience and*

- Remote Sensing, 44(8), 2230–2238. <https://doi.org/10.1109/TGRS.2006.872089>
- Cong, N., Piao, S., Chen, A., Wang, X., Lin, X., Chen, S., Han, S., Zhou, G., & Zhang, X. (2012). Spring vegetation green-up date in China inferred from SPOT NDVI data: A multiple model analysis. *Agricultural and Forest Meteorology*, 165, 104–113. <https://doi.org/10.1016/j.agrformet.2012.06.009>
- Dai, A. (2013). Increasing drought under global warming in observations and models. *Nature Climate Change*, 3(1), 52–58. <https://doi.org/10.1038/nclimate1633>
- de Miranda, J. D., Padilla, F. M., Lázaro, R., & Pugnaire, F. I. (2009). Do changes in rainfall patterns affect semiarid annual plant communities? *Journal of Vegetation Science*, 20(2), 269–276. <https://doi.org/10.1111/j.1654-1103.2009.05680.x>
- Diffenbaugh, N. S., Swain, D. L., & Touma, D. (2015). Anthropogenic warming has increased drought risk in California. *Proceedings of the National Academy of Sciences of the United States of America*, 112(13), 3931. <https://doi.org/10.1073/pnas.1422385112>
- Ehleringer, J. R., Cerling, T. E., & Helliker, B. R. (1997). C4 photosynthesis, atmospheric CO₂, and climate. *Oecologia*, 112(3), 285–299. <https://doi.org/10.1007/s004420050311>
- Fang, Q., Wang, G., Liu, T., Xue, B.-L., & Aa, Y. (2018). Controls of carbon flux in a semi-arid grassland ecosystem experiencing wetland loss: Vegetation patterns and environmental variables. *Agricultural and Forest Meteorology*, 259, 196–210. <https://doi.org/10.1016/j.agrformet.2018.05.002>
- Fay, P. A., Kaufman, D. M., Nippert, J. B., Carlisle, J. D., & Harper, C. W. (2008). Changes in grassland ecosystem function due to extreme rainfall events: Implications for responses to climate change. *Global Change Biology*, 14(7), 1600–1608. <https://doi.org/10.1111/j.1365-2486.2008.01605.x>
- Filippa, G., Cremonese, E., Migliavacca, M., Galvagno, M., Forkel, M., Wingate, L., Tomelleri, E., Morra di Cella, U., & Richardson, A. D. (2016). Phenopix: A R package for image-based vegetation phenology. *Agricultural and Forest Meteorology*, 220, 141–150. <https://doi.org/10.1016/j.agrformet.2016.01.006>
- Gibbens, R. P., & Lenz, J. M. (2001). Root systems of some Chihuahuan Desert plants. *Journal of Arid Environments*, 49(2), 221–263. <https://doi.org/10.1006/jare.2000.0784>
- Gonsamo, A., Chen, J. M., & Ooi, Y. W. (2018). Peak season plant activity shift towards spring is reflected by increasing carbon uptake by extratropical ecosystems. *Global Change Biology*, 24(5), 2117–2128. <https://doi.org/10.1111/gcb.14001>
- Grime, J. P. (2006). *Plant strategies, vegetation processes, and ecosystem properties*. John Wiley & Sons.
- Groisman, P. Y., & Knight, R. W. (2008). Prolonged dry episodes over the conterminous United States: New tendencies emerging during the last 40 years. *Journal of Climate*, 21(9), 1850–1862. <https://doi.org/10.1175/2007JCLI2013.1>
- Guo, Q., Li, S., Hu, Z., Zhao, W., Yu, G., Sun, X., Li, L., Liang, N., & Bai, W. (2016). Responses of gross primary productivity to different sizes of precipitation events in a temperate grassland ecosystem in Inner Mongolia, China. *Journal of Arid Land*, 8(1), 36–46. <https://doi.org/10.1007/s40333-015-0136-7>
- Gutierrez, J. R., Da Silva, O. A., Pagani, M. I., Weems, D., & Whitford, W. G. (1988). Effects of different patterns of supplemental water and nitrogen fertilization on productivity and composition of Chihuahuan Desert annual plants. *American Midland Naturalist*, 119(2), 336–343. <https://doi.org/10.2307/2425816>
- Hegland, S. J., Nielsen, A., Lázaro, A., Bjerknes, A.-L., & Totland, Ø. (2009). How does climate warming affect plant-pollinator interactions? *Ecology Letters*, 12(2), 184–195. <https://doi.org/10.1111/j.1461-0248.2008.01269.x>
- Heisler-White, J. L., Knapp, A. K., & Kelly, E. F. (2008). Increasing precipitation event size increases aboveground net primary productivity in a semi-arid grassland. *Oecologia*, 158(1), 129–140. <https://doi.org/10.1007/s00442-008-1116-9>
- Hernandez-Ramirez, G., Hatfield, J. L., Parkin, T. B., Sauer, T. J., & Prueger, J. H. (2011). Carbon dioxide fluxes in corn-soybean rotation in the midwestern U.S.: Inter- and intra-annual variations, and biophysical controls. *Agricultural and Forest Meteorology*, 151(12), 1831–1842. <https://doi.org/10.1016/j.agrformet.2011.07.017>
- Hinojo-Hinojo, C., Castellanos, A. E., Huxman, T., Rodriguez, J. C., Vargas, R., Romo-León, J. R., & Biederman, J. A. (2019). Native shrubland and managed buffelgrass savanna in drylands: Implications for ecosystem carbon and water fluxes. *Agricultural and Forest Meteorology*, 268, 269–278. <https://doi.org/10.1016/j.agrformet.2019.01.030>
- Hou, E., Litvak, M. E., Rudgers, J. A., Jiang, L., Collins, S. L., Pockman, W. T., Hui, D., Niu, S., & Luo, Y. (2021). Divergent responses of primary production to increasing precipitation variability in global drylands. *Global Change Biology*, 27(20), 5225–5237. <https://doi.org/10.1111/gcb.15801>
- Huxman, T. E., Cable, J. M., Ignace, D. D., Eilts, J. A., English, N. B., Weltzin, J., & Williams, D. G. (2004). Response of net ecosystem gas exchange to a simulated precipitation pulse in a semi-arid grassland: The role of native versus non-native grasses and soil texture. *Oecologia*, 141(2), 295–305. <https://doi.org/10.1007/s00442-003-1389-y>
- Huxman, T. E., Snyder, K. A., Tissue, D., Leffler, A. J., Ogle, K., Pockman, W. T., Sandquist, D. R., Potts, D. L., & Schwinning, S. (2004). Precipitation pulses and carbon fluxes in semiarid and arid ecosystems. *Oecologia*, 141(2), 254–268. <https://doi.org/10.1007/s00442-004-1682-4>
- Jasoni, R. L., Smith, S. D., & Arnone, J. A. III (2005). Net ecosystem CO₂ exchange in Mojave Desert shrublands during the eighth year of exposure to elevated CO₂. *Global Change Biology*, 11, 749–756. <https://doi.org/10.1111/j.1365-2486.2005.00948.x>
- Knapp, A. K., Fay, P. A., Blair, J. M., Collins, S. L., Smith, M. D., Carlisle, J. D., Harper, C. W., Danner, B. T., Lett, M. S., & McCarron, J. K. (2002). Rainfall variability, carbon cycling, and plant species diversity in a mesic grassland. *Science*, 298(5601), 2202–2205. <https://doi.org/10.1126/science.1076347>
- Kurc, S. A., & Small, E. E. (2007). Soil moisture variations and ecosystem-scale fluxes of water and carbon in semiarid grassland and shrubland. *Water Resources Research*, 43(6), W06416. <https://doi.org/10.1029/2006WR005011>
- Liu, W. J., Li, L. F., Biederman, J. A., Hao, Y. B., Zhang, H., Kang, X. M., Cui, X. Y., Wang, Y. F., Li, M. W., Xu, Z. H., Griffin, K. L., & Xu, C. Y. (2017). Repackaging precipitation into fewer, larger storms reduces ecosystem exchanges of CO₂ and H₂O in a semiarid steppe. *Agricultural and Forest Meteorology*, 247, 356–364. <https://doi.org/10.1016/j.agrformet.2017.08.029>
- Milcu, A., Roscher, C., Gessler, A., Bachmann, D., Gockele, A., Guderle, M., Landais, D., Piel, C., Escape, C., Devidal, S., Ravel, O., Buchmann, N., Gleixner, G., Hildebrandt, A., & Roy, J. (2014). Functional diversity of leaf nitrogen concentrations drives grassland carbon fluxes. *Ecology Letters*, 17(4), 435–444. <https://doi.org/10.1111/ele.12243>
- Munson, S. M., & Long, A. L. (2017). Climate drives shifts in grass reproductive phenology across the western USA. *New Phytologist*, 213(4), 1945–1955. <https://doi.org/10.1111/nph.14327>
- Nafus, A. M., McClaran, M. P., Archer, S. R., & Throop, H. L. (2009). Multispecies allometric models predict grass biomass in semidesert rangeland. *Rangeland Ecology & Management*, 62(1), 68–72. <https://doi.org/10.2111/08-003>
- Nakano, T., Nemoto, M., & Shinoda, M. (2008). Environmental controls on photosynthetic production and ecosystem respiration in semi-arid grasslands of Mongolia. *Agricultural and Forest Meteorology*, 148(10), 1456–1466. <https://doi.org/10.1016/j.agrformet.2008.04.011>

- Niu, S., Fu, Z., Luo, Y., Stoy, P. C., Keenan, T. F., Poulter, B., Zhang, L., Piao, S., Zhou, X., Zheng, H., Han, J., Wang, Q., & Yu, G. (2017). Interannual variability of ecosystem carbon exchange: From observation to prediction. *Global Ecology and Biogeography*, 26(11), 1225–1237. <https://doi.org/10.1111/geb.12633>
- Noy-Meir, I. (1973). Desert ecosystems: Environment and producers. *Annual Review of Ecology and Systematics*, 4, 25–51. <https://doi.org/10.1146/annurev.es.04.110173.000325>
- Park, T., Chen, C., Macias-Fauria, M., Tømmervik, H., Choi, S., Winkler, A., Bhatt, U. S., Walker, D. A., Piao, S., Brovkin, V., Nemani, R. R., & Myneni, R. B. (2019). Changes in timing of seasonal peak photosynthetic activity in northern ecosystems. *Global Change Biology*, 25(7), 2382–2395. <https://doi.org/10.1111/gcb.14638>
- Pinheiro, J., Bates, D., DebRoy, S., Sarkar, D., & R Core Team. (2021). *nlme: Linear and nonlinear mixed effects models*. Retrieved from <https://CRAN.R-project.org/package=nlme>
- Polley, H. W., Briske, D. D., Morgan, J. A., Wolter, K., Bailey, D. W., & Brown, J. R. (2013). Climate change and North American rangelands: Trends, projections, and implications. *Rangeland Ecology & Management*, 66(5), 493–511. <https://doi.org/10.2111/REM-D-12-00068.1>
- Potts, D. L., Barron-Gafford, G. A., Butterfield, B. J., Fay, P. A., & Hultine, K. R. (2019). Bloom and Bust: Ecological consequences of precipitation variability in aridlands. *Plant Ecology*, 220(2), 135–139. <https://doi.org/10.1007/s11258-019-00915-2>
- Potts, D. L., Huxman, T. E., Cable, J. M., English, N. B., Ignace, D. D., Eilts, J. A., Mason, M. J., Weltzin, J. F., & Williams, D. G. (2006). Antecedent moisture and seasonal precipitation influence the response of canopy-scale carbon and water exchange to rainfall pulses in a semi-arid grassland. *New Phytologist*, 170(4), 849–860. <https://doi.org/10.1111/j.1469-8137.2006.01732.x>
- Poulter, B., Frank, D., Ciais, P., Myneni, R. B., Andela, N., Bi, J., Broquet, G., Canadell, J. G., Chevallier, F., Liu, Y. Y., Running, S. W., Sitoh, S., & van der Werf, G. R. (2014). Contribution of semi-arid ecosystems to interannual variability of the global carbon cycle. *Nature*, 509(7502), 600–603. <https://doi.org/10.1038/nature13376>
- R Core Team. (2013). *R: A language and environment for statistical computing*. R Foundation for Statistical Computing. Retrieved from <http://www.R-project.org/>
- Reynolds, J. F., Kemp, P. R., Ogle, K., & Fernández, R. J. (2004). Modifying the 'pulse-reserve' paradigm for deserts of north america: precipitation pulses, soil water, and plant responses. *Oecologia*, 141(2), 194–210. <https://doi.org/10.1007/s00442-004-1524-4>
- Roby, M. C., Scott, R. L., & Moore, D. J. P. (2020). High vapor pressure deficit decreases the productivity and water use efficiency of rain-induced pulses in semiarid ecosystems. *Journal of Geophysical Research: Biogeosciences*, 125(10), e2020JG005665. <https://doi.org/10.1029/2020JG005665>
- Sala, O. E., Gherardi, L. A., Reichmann, L., Jobbágy, E., & Peters, D. (2012). Legacies of precipitation fluctuations on primary production: Theory and data synthesis. *Philosophical Transactions of the Royal Society B: Biological Sciences*, 367(1606), 3135–3144. <https://doi.org/10.1098/rstb.2011.0347>
- Schwinning, S., Starr, B. I., & Ehleringer, J. R. (2003). Dominant cold desert plants do not partition warm season precipitation by event size. *Oecologia*, 136(2), 252–260. <https://doi.org/10.1007/s00442-003-1255-y>
- Scott, R. L., Cable, W. L., & Hultine, K. R. (2008). The ecohydrologic significance of hydraulic redistribution in a semiarid savanna. *Water Resources Research*, 44(2), W02440. <https://doi.org/10.1029/2007WR006149>
- Scott, R. L., Hamerlynck, E. P., Jenerette, G. D., Moran, M. S., & Barron-Gafford, G. A. (2010). Carbon dioxide exchange in a semidesert grassland through drought-induced vegetation change. *Journal of Geophysical Research: Biogeosciences*, 115(G3). <https://doi.org/10.1029/2010JG001348>
- Scott, R. L., Jenerette, G. D., Potts, D. L., & Huxman, T. E. (2009). Effects of seasonal drought on net carbon dioxide exchange from a woody-plant-encroached semiarid grassland. *Journal of Geophysical Research: Biogeosciences*, 114(G4), G04004. <https://doi.org/10.1029/2008JG000900>
- Shiklomanov, A. N., Bradley, B. A., Dahlin, K. M., M Fox, A., Gough, C. M., Hoffman, F. M., M Middleton, E., Serbin, S. P., Smallman, L., & Smith, W. K. (2019). Enhancing global change experiments through integration of remote-sensing techniques. *Frontiers in Ecology and the Environment*, 17(4), 215–224. <https://doi.org/10.1002/fee.2031>
- Smith, W. K., Dannenberg, M. P., Yan, D., Herrmann, S., Barnes, M. L., Barron-Gafford, G. A., Biederman, J. A., Ferrenberg, S., Fox, A. M., Hudson, A., Knowles, J. F., MacBean, N., Moore, D. J. P., Nagler, P. L., Reed, S. C., Rutherford, W. A., Scott, R. L., Wang, X., & Yang, J. (2019). Remote sensing of dryland ecosystem structure and function: Progress, challenges, and opportunities. *Remote Sensing of Environment*, 233, 111401. <https://doi.org/10.1016/j.rse.2019.111401>
- Steduto, P., Çetinkökü, Ö., Albrizio, R., & Kanber, R. (2002). Automated closed-system canopy-chamber for continuous field-crop monitoring of CO₂ and H₂O fluxes. *Agricultural and Forest Meteorology*, 111(3), 171–186. [https://doi.org/10.1016/S0168-1923\(02\)00023-0](https://doi.org/10.1016/S0168-1923(02)00023-0)
- Wang, Y. F., Cui, X. Y., Hao, Y. B., Mei, X. R., Yu, G. R., Huang, X. Z., Kang, X. M., & Zhou, X. Q. (2011). The fluxes of CO₂ from grazed and fenced temperate steppe during two drought years on the Inner Mongolia Plateau, China. *Science of the Total Environment*, 410–411, 182–190. <https://doi.org/10.1016/j.scitotenv.2011.09.067>
- Wolledge, J. (1978). The effect of shading during vegetative and reproductive growth on the photosynthetic capacity of leaves in a grass sward. *Annals of Botany*, 42(5), 1085–1089. <https://doi.org/10.1093/oxfordjournals.aob.a085548>
- Wu, D., Zhao, X., Liang, S., Zhou, T., Huang, K., Tang, B., & Zhao, W. (2015). Time-lag effects of global vegetation responses to climate change. *Global Change Biology*, 21(9), 3520–3531. <https://doi.org/10.1111/gcb.12945>
- Xia, J., Niu, S., Ciais, P., Janssens, I. A., Chen, J., Ammann, C., Arain, A., Blanken, P. D., Cescatti, A., Bonal, D., Buchmann, N., Curtis, P. S., Chen, S., Dong, J., Flanagan, L. B., Frankenberg, C., Georgiadis, T., Gough, C. M., Hui, D., ... Luo, Y. (2015). Joint control of terrestrial gross primary productivity by plant phenology and physiology. *Proceedings of the National Academy of Sciences of the United States of America*, 112(9), 2788–2793. <https://doi.org/10.1073/pnas.1413090112>
- Xu, C., Liu, H., Williams, A. P., Yin, Y., & Wu, X. (2016). Trends toward an earlier peak of the growing season in Northern Hemisphere mid-latitudes. *Global Change Biology*, 22(8), 2852–2860. <https://doi.org/10.1111/gcb.13224>
- Yan, D., Scott, R. L., Moore, D. J. P., Biederman, J. A., & Smith, W. K. (2019). Understanding the relationship between vegetation greenness and productivity across dryland ecosystems through the integration of PhenoCam, satellite, and eddy covariance data. *Remote Sensing of Environment*, 223, 50–62. <https://doi.org/10.1016/j.rse.2018.12.029>
- Yang, J., Dong, J., Xiao, X., Dai, J., Wu, C., Xia, J., Zhao, G., Zhao, M., Li, Z., Zhang, Y., & Ge, Q. (2019). Divergent shifts in peak photosynthesis timing of temperate and alpine grasslands in China. *Remote Sensing of Environment*, 233, 111395. <https://doi.org/10.1016/j.rse.2019.111395>
- Zelikova, T. J., Williams, D. G., Hoenigman, R., Blumenthal, D. M., Morgan, J. A., & Pendall, E. (2015). Seasonality of soil moisture mediates responses of ecosystem phenology to elevated CO₂ and warming in a semi-arid grassland. *Journal of Ecology*, 103(5), 1119–1130. <https://doi.org/10.1111/1365-2745.12440>
- Zhang, F., Biederman, J. A., Dannenberg, M. P., Yan, D., Reed, S. C., & Smith, W. K. (2021). Five decades of observed daily precipitation reveal longer and more variable drought events across much of

- the western United States. *Geophysical Research Letters*, 48(7), e2020GL092293. <https://doi.org/10.1029/2020GL092293>
- Zhang, F., Biederman, J. A., Pierce, N. A., Potts, D. L., Devine, C. J., Hao, Y., & Smith, W. K. (2021). Data from: Precipitation temporal repackaging into fewer, larger storms delayed seasonal timing of peak photosynthesis in a semi-arid grassland. *University of Arizona Research Data Repository*, <https://doi.org/10.25422/azu.data.16823602>
- Zhou, Y.-Z., & Jia, G.-S. (2016). Precipitation as a control of vegetation phenology for temperate steppes in China. *Atmospheric and Oceanic Science Letters*, 9(3), 162–168. <https://doi.org/10.1080/16742834.2016.1165594>
- Zuazo, V. H. D., & Pleguezuelo, C. R. R. (2009). Soil-erosion and runoff prevention by plant covers: A review. In E. Lichtfouse, M. Navarrete, P. Debaeke, S. Véronique, & C. Alberola (Eds.), *Sustainable agriculture* (pp. 785–811). Springer. https://doi.org/10.1007/978-90-481-2666-8_48

SUPPORTING INFORMATION

Additional supporting information may be found in the online version of the article at the publisher's website.

How to cite this article: Zhang, F., Biederman, J. A., Pierce, N. A., Potts, D. L., Devine, C. J., Hao, Y., & Smith, W. K. (2021). Precipitation temporal repackaging into fewer, larger storms delayed seasonal timing of peak photosynthesis in a semi-arid grassland. *Functional Ecology*, 00, 1–13. <https://doi.org/10.1111/1365-2435.13980>